

Photo-electrochemical performance of $\text{Cd}_{1-x}\text{Pb}_x\text{S}$ ($0 \leq x \leq 1$) thin filmsM.A. Barote^a, S.S. Kamble^{b,*}, L.P. Deshmukh^c, E.U. Masumdar^d^aDepartment of Physics, Azad College, Ausa -413 520, M.S., India^bBharat-Ratna Indira Gandhi College of Engineering, Kegaon, Solapur, M.S., India^cThin Films and Solar Studies Research Laboratory, Department of Physics, Solapur University, Solapur -413 255, M.S., India^dThin Film Research Laboratory, Rajarshi Shahu Mahavidyalaya, Latur, M.S., India

Received 10 July 2012; received in revised form 27 July 2012; accepted 27 July 2012

Available online 4 August 2012

Abstract

This paper discusses chemical synthesis of $\text{Cd}_{1-x}\text{Pb}_x\text{S}$ ($0 \leq x \leq 1$) thin film layers and their photo-electrochemical properties with special reference to PEC parameters. Previously optimized conditions were used for the deposition. The electrode/electrolyte interfaces were then formed between the $\text{Cd}_{1-x}\text{Pb}_x\text{S}$ thin film layers and a sulphide/polysulphide (1 M) redox couple and investigated through the various photo-electrochemical (PEC) properties to assess suitability to convert solar energy into electrical energy.

Increase in short circuit current (I_{sc}) and open circuit voltage (V_{oc}) was observed with increased composition and attain maximum at $x=0.175$. Power conversion efficiency and fill factor were found to be 0.163% and 46.2% respectively for the composition parameter $x=0.175$.

© 2012 Elsevier Ltd and Techna Group S.r.l. All rights reserved.

Keywords: Thin films; Chemical deposition; $\text{Cd}_{1-x}\text{Pb}_x\text{S}$; Solar cell

1. Introduction

Maximum utilization of solar spectrum and stability against anodic reactions forms a constraint over PEC cell formation. The efficiency and stability of PEC cell depends on the material properties and preparative conditions [1,2]. Recently CdS and PbS thin films have attracted spotlight in optoelectronic applications owing to the features viz. high absorption coefficient, ability of band gap engineering, long-term optoelectronic stability and ease of synthesis via range of deposition techniques [3–5].

By considering the increasing demands for reliable and cost-competitive means of thin film synthesis for industrial escalation we have adopted inexpensive novel route of chemical deposition for present system. Chemical deposition is the occurrence of a moderately slow chemical reaction in solution bath that results into a solid product on the immersed substrate [4]. Involvement of low processing temperature, inexpensive equipment and ease of deposition on any size and shape of substrate mould chemical route as

an ideal for industrial adaptation. Nevertheless, chemical route has earned core place in the flexible electronics due to feasibility of routine deposition of nano-structured films and owing to above strong advantages. Thus, being promising candidate for optoelectronic device applications, CdS and its Pb-doped derivative thin films were obtained by using chemical deposition route.

2. Experimental details

2.1. Preparation of $\text{Cd}_{1-x}\text{Pb}_x\text{S}$ thin film electrodes

$\text{Cd}_{1-x}\text{Pb}_x\text{S}$, ($0 \leq x \leq 1$) thin film layers have been prepared on FTO coated glass substrates by inexpensive, novel chemical deposition route. Optimized parameters (pH = 10.5 ± 0.1 , temperature = 80°C , time = 60 min, rotation speed = 65 rpm) were used for chemical synthesis of $\text{Cd}_{1-x}\text{Pb}_x\text{S}$ thin film layers [6].

2.2. Fabrication and characterization of PEC cell

PEC cells were fabricated using a classical 3-electrode system. The as-prepared naked $\text{Cd}_{1-x}\text{Pb}_x\text{S}$ films were used

*Corresponding author. Tel.: +91 9970 836665.

E-mail address: shrishail_kamble@yahoo.co.in (S.S. Kamble).

as an active photo-electrode; impregnated graphite and a saturated calomel electrode (SCE) were used as the counter and reference electrodes, respectively. Aq. 1 M polysulphide ($\text{NaOH} + \text{Na}_2\text{S} + \text{S}$) was used as a redox couple. A 100 W tungsten filament lamp was used as an illumination source. The distance between photo-electrode and counter electrode was 0.3 cm and the sample area was defined with a common epoxy resin.

3. Results and discussion

Earlier investigations [6,7] on $\text{Cd}_{1-x}\text{Pb}_x\text{S}$ ($0 \leq x \leq 1$) thin films revealed enhancement in electrical conductivity with the assimilation of Pb in CdS host lattice up to $x=0.175$.

3.1. Current voltage characteristics

The current voltage (IV) measurements are generally used to focus on the charge transfer mechanism at the electrode/electrolyte interface. PEC cell formed with general configuration $\text{Cd}_{1-x}\text{Pb}_x\text{S}/1\text{ M } (\text{NaOH} + \text{Na}_2\text{S} + \text{S})/\text{graphite}$ was used to record IV characteristics for all the electrodes. Current transport mechanism through electrode/electrolyte interface can be explained on the basis of Butler–Volmer relation,

$$I = I_0 \{ \exp[(1-\beta)VF/RT] \exp[\beta VF/RT] \}$$

where I_0 is the equilibrium exchange current density, V is the over voltage, β is the symmetry factor, R is the universal gas constant and, F is the Faraday constant.

When symmetry factor is $\beta=0.5$, it corresponds to the presence of a symmetrical barrier height and yields a symmetrical I – V curve. It has been seen that the junctions are rectifying in nature with asymmetric nature of I – V plot (Fig. 1A and B) in forward bias and reverse bias, highlighting the Faradiac rectification [8].

The junction ideality factor in dark (n_d) and under illumination (n_L) was then determined for all the cells from the slopes of $\log I$ vs. V plots. Fig. 2A and B reveals

the linear behaviour of $\log I$ vs. V in dark and under illumination. n_d and n_L values (Table 1) were found to be higher than expected indicating the influence of various recombination mechanisms on current transfer and series resistance effect as a consequence of surface states [9–11].

3.2. Capacitance voltage characteristics

The most common capacitance measurement on the PEC cell is capacitance voltage (CV) measurement, which can be used to estimate the donor concentration (N_D) using the following equation:

$$\frac{1}{C_s^2} = \left[\frac{2}{\epsilon_0 \epsilon_s q N_D} \right] \left[V - V_{fb} - \left(\frac{kT}{q} \right) \right]$$

where C_s is the space charge capacitance, V_{fb} is the flatband potential, ϵ_0 is the permittivity of free space, ϵ_s is the static permittivity of the semiconductor and q is the charge on electrons.

The donor concentration can be calculated from the slope of the $1/C^2$ vs. V curve. Fig. 3A reveals the Mott–Schottky plot for $\text{Cd}_{1-x}\text{Pb}_x\text{S}/\text{sulphide}/\text{polysulphide}$ electrolyte system in the dark, and the flatband potential can be determined by extrapolation to $C_s=0$.

Flatband potential (V_{fb}), is a measure of maximum open-circuit voltage attainable from the cell and it gives the information on relative position of the fermi level in terms of the band bending caused by surface interactions [12].

3.3. Barrier height measurement

The barrier height (Φ_b) is the energy difference between the edge of conduction band and the redox fermi level of the electrolyte. The reverse saturation current flowing through junction is related to temperature by:

$$I_0 = AT^2 \exp(\Phi_b/kT)$$

where A is the Richardson constant, k is the Boltzmann constant, Φ_b is the barrier height.

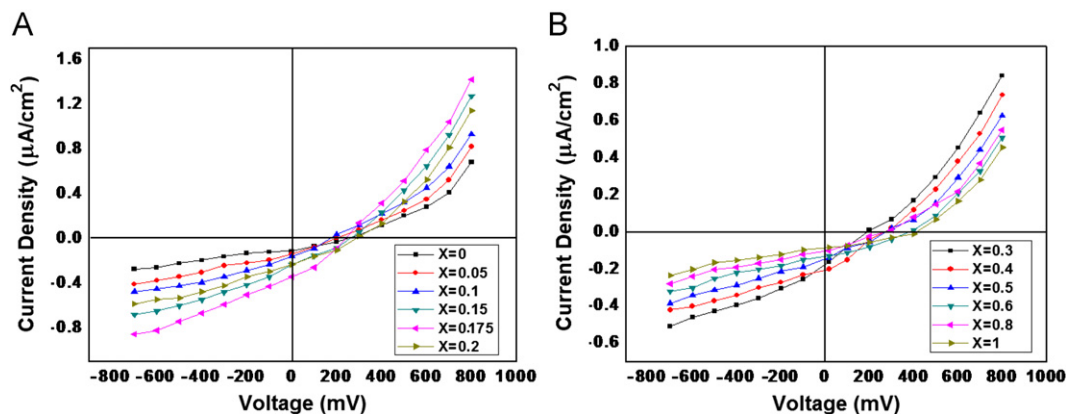


Fig. 1. (A) IV characteristics of $\text{Cd}_{1-x}\text{Pb}_x\text{S}/(1\text{ M NaOH}+1\text{ M Na}_2\text{S}+1\text{ M S})/\text{C}$ PEC cell in dark. (B) IV characteristics of $\text{Cd}_{1-x}\text{Pb}_x\text{S}/(1\text{ M NaOH}+1\text{ M Na}_2\text{S}+1\text{ M S})/\text{C}$ PEC cell under illumination.

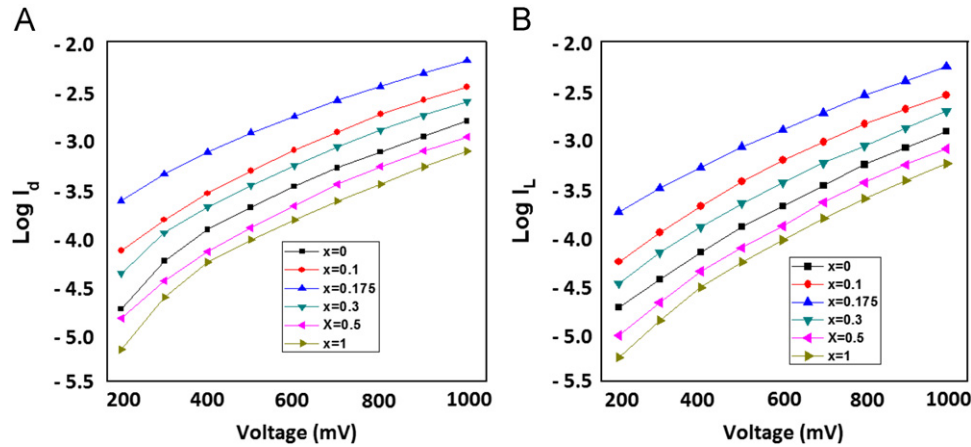


Fig. 2. (A) Variation of $\log I_d$ vs. V for $\text{Cd}_{1-x}\text{Pb}_x\text{S}/(1 \text{ M NaOH}+1 \text{ M Na}_2\text{S}+1 \text{ M S})/\text{C}$ PEC cells. (B) Variation of $\log I_L$ vs. V for $\text{Cd}_{1-x}\text{Pb}_x\text{S}/(1 \text{ M NaOH}+1 \text{ M Na}_2\text{S}+1 \text{ M S})/\text{C}$ PEC cell.

Table 1

Various photo-electrochemical (PEC) performance parameters of $\text{Cd}_{1-x}\text{Pb}_x\text{S}$ ($0 \leq x \leq 1$) thin films.

Composition parameter (x)	n_d	n_L	I_{sc} ($\mu\text{A}/\text{cm}^2$)	V_{oc} (mV)	R_s (Ω)	R_{sh} ($\text{k}\Omega$)	$\eta\%$	$ff\%$	Φ_b (eV)
0	2.18	1.76	224	158	350	2.77	0.049	36.2	0.832
0.05	2.12	1.67	248	173	328	4.62	0.065	38.1	0.787
0.1	2.07	1.61	277	195	309	5.26	0.092	42.3	0.711
0.175	1.89	1.52	368	240	233	7.41	0.163	46.2	0.569
0.3	2.93	1.98	289	203	318	5.17	0.098	41.7	0.681
0.5	3.02	2.06	272	180	332	4.05	0.079	40.4	0.724
1	3.27	2.28	235	155	523	2.61	0.041	36.8	0.843

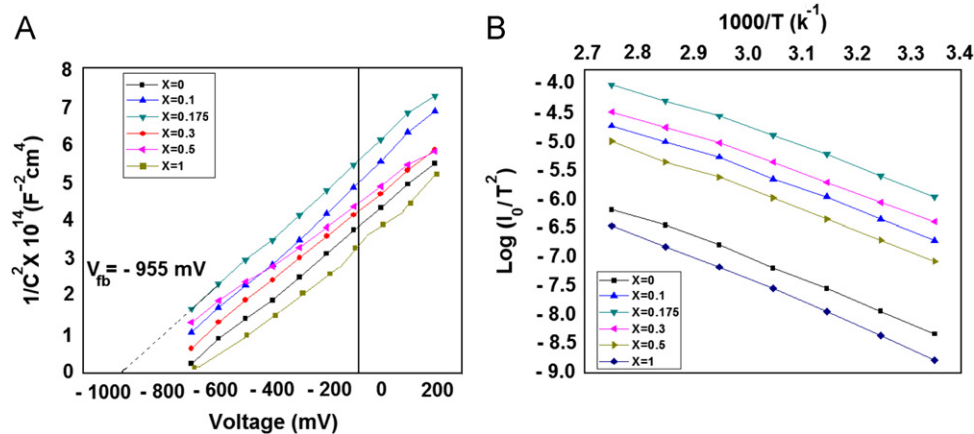


Fig. 3. (A) Mott-Schottky plots for $\text{Cd}_{1-x}\text{Pb}_x\text{S}/(1 \text{ M NaOH}+1 \text{ M Na}_2\text{S}+1 \text{ M S})/\text{C}$ PEC cells. (B) Plot of $\log (I_0/T^2)$ with $1000/T$ for $\text{Cd}_{1-x}\text{Pb}_x\text{S}/(1 \text{ M NaOH}+1 \text{ M Na}_2\text{S}+1 \text{ M S})/\text{C}$ PEC cells.

Barrier height (Φ_b) was determined from the slope of linear regions of $\log (I_0/T^2)$ with $1000/T$ plots (Fig. 3B). Non-linearity of plots observed in high temperature region can be attributed to the Pool-Frankel type of mechanism [11,12].

3.4. Photovoltaic power output

Fig. 4A shows the photovoltaic power output characteristics under forward bias and constant illumination of $25 \text{ mW}/\text{cm}^2$. It is found that, both short circuit current (I_{sc}

is the current through the solar cell when the voltage across the solar cell is zero) and open circuit voltage (V_{oc} is the maximum voltage across the solar cell when the current through the solar cell is zero) are increased with increased Pb concentration and attain a maximum value at $x=0.175$.

Performance of the PEC cell can be estimated using precise values of the fill factor (ff) and the conversion efficiency (η)

$$\eta = \frac{I_{sc} V_{oc} ff}{P_{input}} \times 100$$

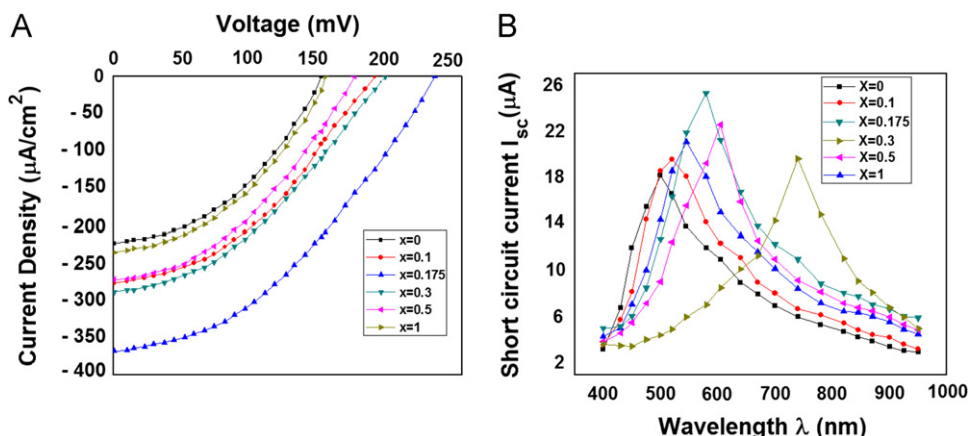


Fig. 4. (A) Power output characteristics for $\text{Cd}_{1-x}\text{Pb}_x\text{S}/(1 \text{ M NaOH}+1 \text{ M Na}_2\text{S}+1 \text{ M S})/\text{C}$ PEC cell. (B) Spectral response curves of $\text{Cd}_{1-x}\text{Pb}_x\text{S}/(1 \text{ M NaOH}+1 \text{ M Na}_2\text{S}+1 \text{ M S})/\text{C}$ PEC cells.

$$ff = \frac{V_{max}I_{max}}{I_{sc}V_{oc}}$$

where, P_{input} is the power density of incident radiation, I_{max} is the maximum current obtained from PEC cell, V_{max} is the maximum voltage obtained from PEC cell.

The fill factor is directly affected by the values of the cell's series (R_s) and shunt resistances (R_{sh}). To estimate R_s and R_{sh} , a straightforward technique is used i.e., by measuring the slope of power output characteristics.

Photovoltaic efficiency was found to be increased with the composition parameter ' x ' up to 0.175. This synchronised increase in efficiency is attributed to the increment in short circuit current, open circuit voltage and enhanced flatband potential due to increased grain size and surface defects [6,7].

3.5. Spectral response characteristics

The spectral response measurement is essential for understanding efficiency of a PEC cell to convert incident radiation into current at various wavelengths. The conversion efficiency in units of electron-hole pairs collected per incident photon is computed from the measured spectral responsivity as a function of wavelength. Spectral response (Fig. 4B) of the PEC cell formed with CdPbS thin films is studied by measuring short circuit current (I_{sc}) as a function of wavelength (λ). It is perceived that, the photocurrent is at maximum for composition parameter $x=0.175$; indicating low population of surface defects in the space charge region. Higher photocurrent in this case can be correlated to the shift of spectral response towards higher wavelength and reduced series cell resistance. Whereas, decreased photocurrent on shorter wavelength side is attributed to the incident radiation absorption in electrolyte and recombination of the minority carriers presumably mediated by the electronic states in the band gap region [13,14].

4. Conclusion

- The $\text{Cd}_{1-x}\text{Pb}_x\text{S}$ ($0 \leq x \leq 1$) thin films have been deposited using novel chemical deposition route.
- Maximum conversion efficiency of 0.163% is feasible with as-prepared $\text{Cd}_{1-x}\text{Pb}_x\text{S}$ thin film layers.
- Synchronized increase in efficiency is correlated with the enhanced short-circuit current, open-circuit voltage and flatband potential.
- Highest value of flatband potential (955 mV) was observed for the cell with electrode composition $x=0.175$.

References

- [1] A.A. Yadav, M.A. Barote, E.U. Masumdar, Photoelectrochemical properties of spray deposited n -CdSe thin films, *Solar Energy* 84 (2010) 763–770.
- [2] V.M. Bhuse, Photo-electrochemical properties of $\text{Cd}_{1-x}\text{Hg}_x\text{Se}$ thin films, *Materials Chemistry and Physics* 106 (2007) 250–255.
- [3] A.A. Yadav, M.A. Barote, E.U. Masumdar, Studies on nanocrystalline cadmium sulphide (CdS) thin films deposited by spray pyrolysis, *Solid State Sciences* 12 (2010) 1173–1177.
- [4] S.T. Mane, S.S. Kamble, S.A. Lendave, L.P. Deshmukh, Aqueous alkaline chemical bath deposition of $\text{Cd}_{1-x}\text{Co}_x\text{S}$ thin films, *Materials Letters* 67 (2012) 373–375.
- [5] A.N. Chattarki, S.S. Kamble, L.P. Deshmukh, Role of pH in aqueous alkaline chemical bath deposition of lead sulfide thin films, *Materials Letters* 67 (2012) 39–41.
- [6] M.A. Barote, S.S. Kamble, A.A. Yadav, R.V. Suryavanshi, L.P. Deshmukh, E.U. Masumdar, Thickness dependence of $\text{Cd}_{0.825}\text{Pb}_{0.175}\text{S}$ thin film properties, *Materials Letters* 78 (2012) 113–115.
- [7] M.A. Barote, A.A. Yadav, L.P. Deshmukh, E.U. Masumdar, Synthesis and of chemically deposited $\text{Cd}_{1-x}\text{Pb}_x\text{S}$ thin films, *J. Non-Oxide Glasses* 3 (2010) 151.
- [8] M.T. Gutiérrez, J. Ortega, Influence of chemical and photoelectrochemical etching on the n - $\text{CdSe}_{0.65}\text{Te}_{0.35}$ polycrystalline thin films: Application in the PEC cells, *Solar Energy Materials* 20 (1990) 387–394.
- [9] M.A. Butler, Photoelectrolysis and physical properties of the semi-conducting electrode WO_2 , *Journal of Applied Physics* 48 (5) (1977) 1914–1920.

- [10] A. Aruchamy, G. Aravamudan, G.V. Subba Rao, Semiconductor based photoelectrochemical cells for solar energy conversion-an overview, *Bulletin of Materials Science* 4 (1982) 483–526.
- [11] P.K. Mahapatra, A.R. Dubey, Photoelectrochemical behaviour of mixed polycrystalline *n*-type CdS-CdSe electrodes, *Solar Energy Materials and Solar Cells* 32 (1994) 29–35.
- [12] L.P. Deshmukh, G.S. Shahane, CdS_{1-x}Se_x thin film electrodes: an electrochemical photovoltaic study, *International Journal of Electronics* 83 (1997) 341–350.
- [13] A. Heller, K.C. Chang, B. Miller, Spectral response and efficiency relations in semiconductor liquid junction solar cells, *Journal of the Electrochemical Society* 124 (1977) 696–700.
- [14] D.S. Ginley, M.A. Butler, The photoelectrolysis of water using iron titanate anodes, *Journal of Applied Physics* 48 (5) (1997) 2019–2021.